17th World Conference on Earthquake Engineering, 17WCEE

Sendai, Japan - September 13th to 18th 2020

Analytical Study on 3-D Shake Table Test Results for Full-Scale 5-Story Steel Building with Steel Dampers

H. Yamagiwa[(1)], K. Kasai[(2)], Y. Baba[(3)], Y. Matsuda[(4)]

[(1)] *Technical Research Institute, Okumura Corporation, Japan, hajime.yamagiwa@okumuragumi.jp*
[(2)] *Specially Appointed Prof., Tokyo Institute of Technology, Japan, kasai.k.ac@m.titech.ac.jp*
[(3)] *Yasui Architects & Engineers, Inc., Japan, yuki-baba@yasui-archi.co.jp*
[(4)] *Assistant Prof., Tokyo University of Science, Japan, matsuda_y@rs.tus.ac.jp*

Abstract

Realistic 3-D shaking table tests using the large scale facility of E-Defense in Japan were conducted for full-scale 5-story steel frame building specimen (Fig.0-1) with/without dampers in order to evaluate the anti-seismic performance against ground motions of scales ranging from minor to catastrophic levels. The building was tested repeatedly, inserting and replacing each of four different types of dampers, steel, viscous, oil, and viscoelastic dampers. This paper discuss the detailed 3-D analytical modeling for the frame with steel dampers.

The steel damper employed here is the buckling-restrained brace composed of low yield strength steel (LY225). Since the characteristics of the damper have the strain rate dependency, the damper is modeled with a parallel three elements: an elasto-plastic elements of steel, a nonlinear viscous element of steel, and a linear viscoelastic element of filler (butyl rubber).

First, we built 3-D analytical frame model including the above steel damper model to simulate the responses of the specimen. This model simulated the experimental results of whole response of the building and local behavior of steel dampers with high accuracy. In the general design model, the axial force generated in the beam owing to the dampers cannot be simulated when the rigid floor assumption is used to slab. On the other hand, when we use the suggested analysis model of slab (Fig.0-2), it was confirmed that the transfer of building inertial force to the damped bay through the slab can be simulated and the axial force in the beam can be evaluated.

Second, we evaluated the degree of effect to whole response of the building using nine different analysis models considering the existence of slabs, beam hunched parts, panel zones, non-structural components, and variation of modeling in steel dampers. As a result, we confirmed that the effects of slab and non-structural components are not small.

Keywords: Passive control, Full-scale test, Shaking table, Steel damper, Frame analysis

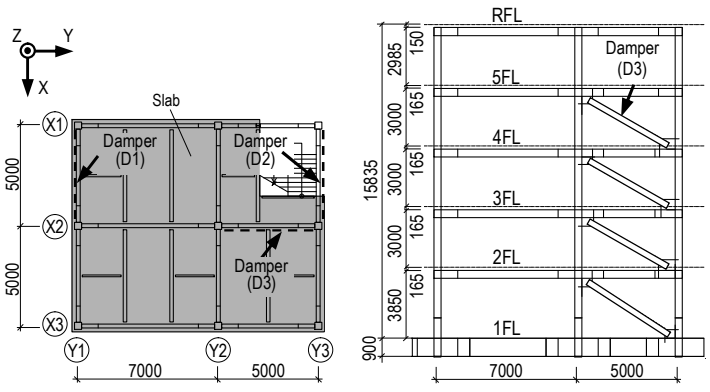

(a) typical floor plan (b) X2 frame

Fig.0-1 – Summary of steel building specimen

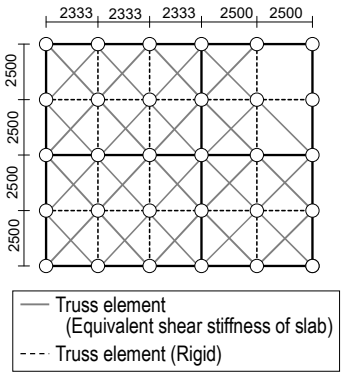

Fig.0-2 – Analysis model of slab

1. Introduction

1.1 Background

In recent years, various types of dampers have been developed and applied to many buildings. However, damping effects of actual buildings have been evaluated only in small range motions due to micro-tremor measurements or vibration generator tests. Therefore, it is possible that actual buildings may have been designed with many uncertainties about whether modeling of dampers and building components have been properly performed. So, it was necessary to make clear those effects in detail at full-scale level.

Therefore, realistic 3-D shaking table tests using the large scale facility of E-Defense in Japan were conducted for full-scale 5-story steel frame building specimen (Fig.1) with/without dampers. Representative four different types of dampers, steel, viscous, oil, and viscoelastic dampers were alternatively attached to the frame, and small- to full-scale of the ground motions recorded at JR Takatori station during the 1995 Great Hansin earthquake were applied to the test specimen. After finishing the test series, the frame without dampers were also tested using the same motion but scaled to 0.7 times, due to the concerns of safety. In these tests, more than 1,400 sensors were used, and accurate global and local data was obtained. Through these tests, we were able to demonstrate the damper's performance for small to large earthquakes, and made various discoveries regarding damper's effects. (without damper: [1], with dampers: [2]~[5], of all: [8])

On the other hand, since full-scale tests are not easy, general consideration of damper's performance requires response prediction by accurate analysis instead of tests. In particular, practical analysis models that simulate members and joints by line and spring elements will be used in design. And, if they have sufficient accuracy, it is considered to be important for practical and various studies. For the accuracy verification of analysis models, global and local realistic data obtained from the above full-scale tests are the most effective data.

In addition, the high-precision analysis can reproduce behaviors that could not be measured by the enormous number of sensors due to the large scale of the specimen. Furthermore, tests that were impossible due to safety and loading capacity can be reproduced. Using the proven analysis method as a benchmark, it is also possible to verify various types of modeling, and make proposals that contribute to improving the accuracy of general modeling.

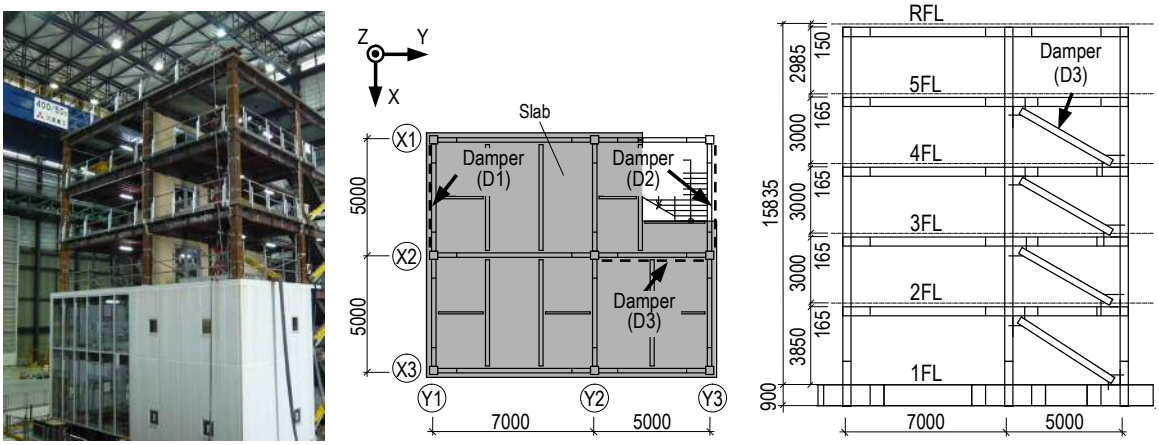

(a) Exterior view (b) Typical floor plan (c) X2 frame

Fig. 1 – Summary of steel building specimen (with steel dampers)

1.2 Objectives and Scopes

Based on the above background, in reference [6], the 3-D frame model using line and spring was constructed for simulating full-scale tests without dampers. In this reference, test results without dampers were reproduced with high accuracy for both global and local behaviors.

This paper focuses on the full-scale tests with steel dampers. The scope of this paper is as follows:

Chapter 2 gives the overview of the specimen used in the tests, outline of the analysis model focusing on modeling of the steel damper, and characteristics of selected input seismic motion. Chapter 3 demonstrates excellent accuracy of analysis for reproducing the test results from global to local responses, and discusses the effects of slab modeling on the analytical results. Chapter 4 discusses effects of partially changing elements and their parameters for the model on the analytical results. Finally, chapter 5 summarizes the results of the study.

2. Outline of Analysis

2.1 Modeling of Frame Portion

The details of the analysis model of frame portions of this specimen are given in reference [6], and the following summarize the frame model:

The column and beam are simulated by elasto-plastic element considering axial, bending and shear actions. In consideration of stiffness of the beam with horizontal haunch and/or gusset plate, the beam is divided into sections within the span and cross-sectional properties is input to each sections (Fig.2 (a)). The post-yield stiffness is set to 0.01 times the elastic stiffness. The yield strength is the value reflecting steel yield stress and concrete compressive strength obtained from the material tests. The panel zone is simulated by the rotational spring element having rotational stiffness (Fig.2 (b)), and its yield strength calculated based on the shape and material strength. The non-structural component is modeled by considering the experimental relationship between the story drift and total shear force of various non-structural components which are estimated by subtracting sum of damper forces and column shear forces from the story shear force estimated from the measured inertia force. It's simulated slip behavior of the non-structural component by reflecting stiffness reduction caused by the repeated shaking tests. In addition, the horizontal negative stiffness springs are connected to each floor for simulating P-δ effects. The weight is lumped to the joints between the beams on each floor according to contributory area of each column. The horizontal mass of each floor is adjusted so that mass moment of inertia and total mass of each story are equal to those in the tests. The damping ratio of the frame is set to Rayleigh-type damping determined from mode periods and damping

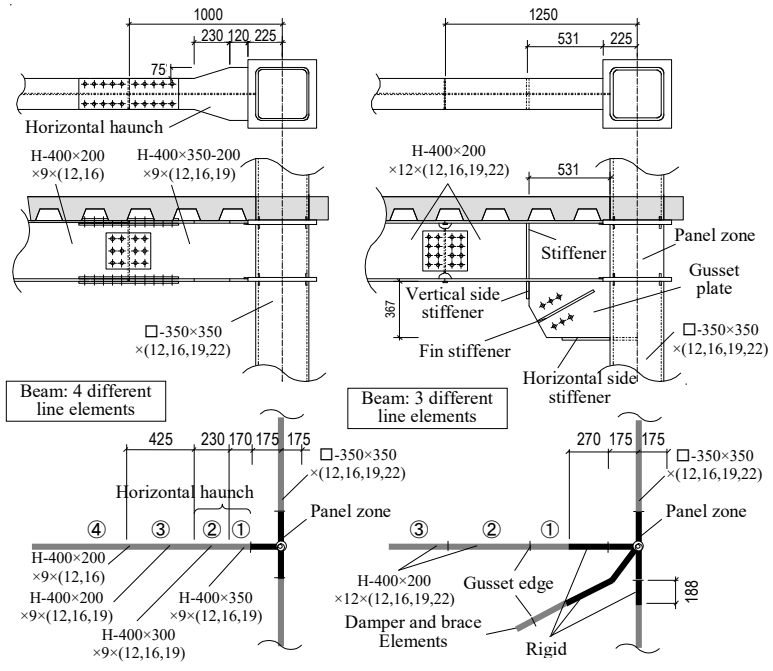

(a) Column, beam, and gusset joint
(left:undumped frame, right:dumped frame)

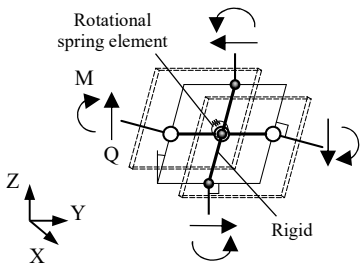

(b) Panel zone

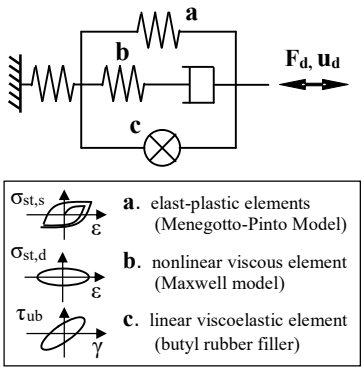

(c) Steel damper

Fig. 2 – Analysis model for each elements

ratios in each of 1st and 2nd modes obtained from the test results of the specimen without damper at the 20% Takatori motion (both of damping ratios are about 1.3%).

The weight of the specimen with steel dampers was about 50kN lighter than that of the specimen without damper because ceiling was not attached during the tests of the specimen with dampers, and it was about 77kN heavier because of added 12 dampers, and increased about 27kN in total (total weight 4,906kN). The notations of columns (C1 to C9) and beams (B12 to B98) are defined in the floor plan of Fig.1 (b).

The steel damper is a buckling-restrained brace. To prevent buckling, the mortar and the steel pipe restrain the steel plate that receives axial force. The steel plate is low yield strength steel (LY225), and filler (butyl rubber) applied between the steel plate and the mortar. The elastic part of the steel plate has a cruciform section, and the elasto-plastic part has a flat section. The cross section of the former is about 2.7 times that of the latter.

In modeling the specimen without damper, the composite beam is considered based on the shake table test results: The strain of the beam cross section was measured in two sections at the same span, the neutral axis location at the positive and maximum negative bending moments at each position is calculated, and the average height of these cases of neutral axis locations is used for the analysis models of beams. Then, assuming that the strain distribution keeps plane in the cross section, the effective width of the slab is obtained by balancing forces, and the moment of inertia of the beam in the analysis model can determined. However, when dampers are attached, the axial force is caused for the beam attached dampers, and it shifts the neutral axis location. In such a case, focusing on the fact that phases of the axial force and the bending moment are different, strains due to bending moment were extracted from measured strains, and used to determine the moment of inertia of the composite beam (method shown in reference [7]).

2.2 Modeling of Steel Damper

Total of 12 dampers were attached to 3 frames in the 1st to 4th floors (Fig.1). The X-direction dampers were attached to Y1 and Y3 frames, called D1 and D2 dampers. The Y-direction dampers were attached to X2 frame, called D3 dampers, and the capacity of D3 dampers were about twice that of D1 and D2 dampers. Since the characteristics of the steel damper have the strain rate dependency, the damper is modeled with parallel three elements: an elasto-plastic element of steel, a nonlinear viscous element of steel, and a linear viscoelastic element of filler (Fig.2 (c)).

2.3 Input Seismic Waves

In the tests, The JR Takatori ground motion (hereinafter called “Takatori motion”) adjusted by various scaling factors (e.g., 15%, 40%, 50%, 70%, 100%) were used. This is one of the strongest motions recorded during the 1995 Kobe Earthquake. Also, in the analytical study to reproduce the tests described later, the absolute acceleration records of X, Y, and Z directions in 1/100 second increment obtained at the center of the specimen on the shaking table from the tests are used. In addition, slight rocking of the shaking table occurred in the tests, so the acceleration record of the rotation on the shaking table is additionally input to the analysis model. This rocking motion is described in detail in reference [9].

Fig.3 shows the acceleration and displacement response spectra of 100% Takatori motion. The damping ratio of 2% is used. In the tests, WN(white noize) motion was input after 40% Takatori motion, and the 1st mode period at WN motion is almost equal to the elastic 1st mode period of the analysis model for 100% Takatori motion (hereinafter called “analysis period”). On the other hand, the 1st mode period at 100% Takatori motion test appears to be 10% longer than the analysis period due to the nonlinearity of the damper. Although not shown in Fig.3, the 1st mode period at 15% Takatori motion is about 3% shorter than the analysis period because of less damage to non-structural materials and slabs. Around these periods, the displacement response spectrum of 100% Takatori motion slightly rises to the right (Fig.3 left), while the acceleration response spectrum of 100% Takatori motion slightly drops to the right (Fig.3 right) in both X and Y directions.

3. Evaluation of Tests by Analysis

3.1 Global Responses

The time history response analysis was performed using the 15%, 50%, and 100% Takatori motions. Hereinafter, comparison between the test results and the analysis results is described. Here, when analyzing for the 50% and 100% Takatori motions, respectively, analysis using 40% and 70% Takatori motions conducted in advance, in order to more faithfully reproduce the stiffness reduction due to damage of non-structural components etc. The time step size for the analysis is 1/1000 second, and Newmark β method (β=1/4 : average acceleration method) is used as the numerical integration method. In addition, Newton-Raphson method is used as the convergence calculation method at the time of nonlinearity.

Fig.4 shows the maximum values of drift ratio, absolute acceleration, and shear force of each story. Highly accurate analysis results are obtained regardless of input motion level. Fig.5 shows the displacement

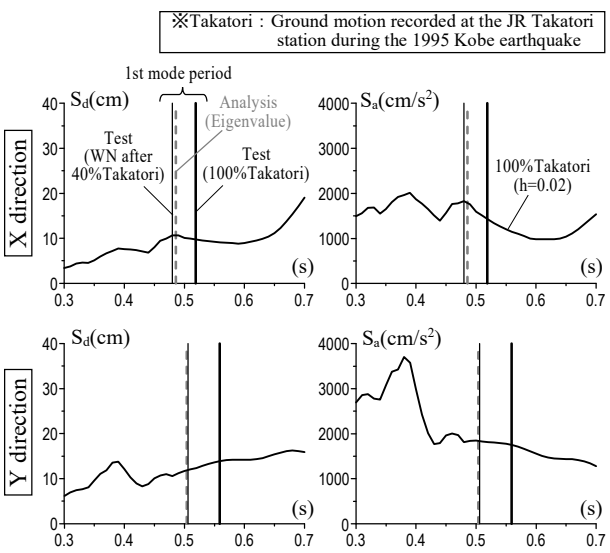

Fig. 3 – Acceleration and displacement response spectra (100%Takatori , h=0.02)

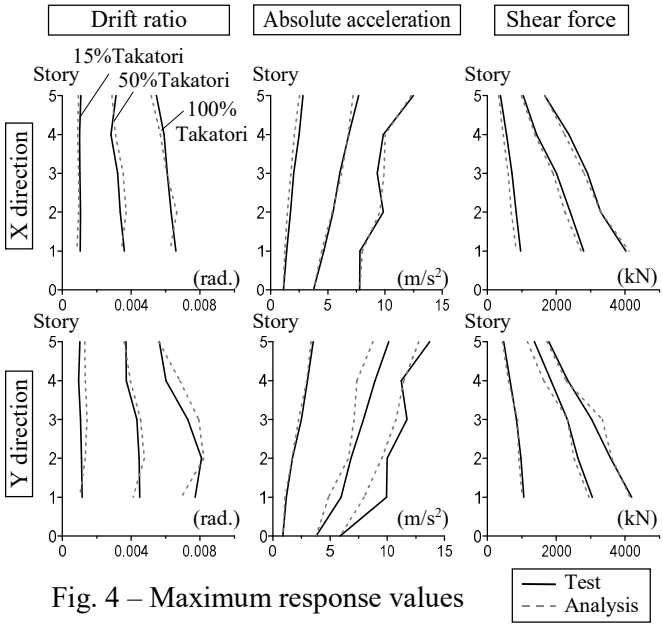

Fig. 4 – Maximum response values

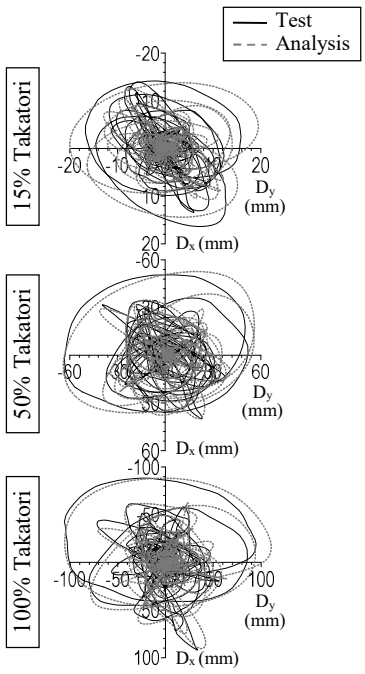

Fig. 5 – Displacement orbit (relative displacement from base to top)

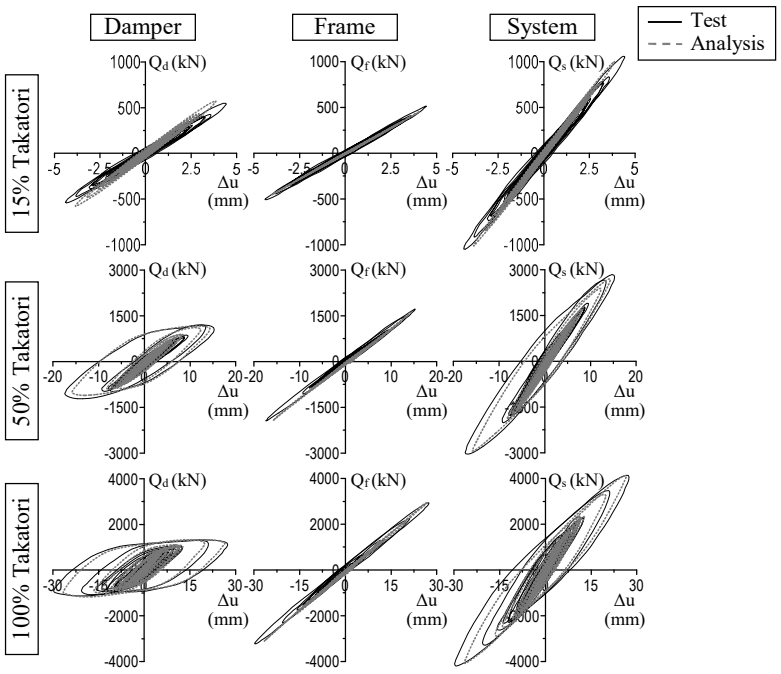

Fig. 6 – Shear force - deformation relationship of damper, frame, and system (Y direction, 1st floor)

orbits (relative displacement from base to top). Although the displacement of Y-direction at 15% Takatori motion tends to be overestimated, 2-D complicated motions of the specimen can be reproduced by the analysis at any input motion level. Fig.6 shows the relationship between shear force and deformation of the damper (Q_d -Δu), the frame (Q_f -Δu), and the system (Q_s -Δu). When 15% Takatori motion is input, the damper and the frame stiffness is almost the same, but as the input motion level increases, the ratio of shear force of the damper decreases because the damper yields. This tendency is well reproduced by the analysis.

3.2 Local Responses

Fig. 7 shows the relationship between damper axial forces and damper strokes. When 15% Takatori motion is input, the hysteresis curve shapes almost straight in general because the damper does not yield, but the figure shows thin loops in the hysteresis curve. It is due to the viscoelastic behavior of filler and the velocity dependency of the steel in dampers, and the tendency can be reproduced by the analysis. The modeling of the steel damper is found to accurately simulate the dynamic characteristics. Although the damper yields and the hysteresis loop becomes fatter with increase of input motion level, hysteresis of all of D1, D2 and D3 dampers are well reproduced by the analysis. Fig.8 shows the energy absorption of all dampers. Regardless of input motion level from the initial time, the analysis can evaluate the tests with high accuracy, indicating that reliability of the analysis model of the steel damper (Fig.2 (c)) is very high.

Unless otherwise specified, the results for the 100% Takatori motion are described below.

Fig.9 shows the time history of the 1st floor column moment. In the X and Y directions, the moments at the column base and top are both accurately simulated by the analysis. Fig.10 shows the time history of the column axial force. Although the column with damper transmits the damper force, the axial force of the column with damper (Fig.10 (b)) is larger than that of the column without damper (Fig.10 (a)), and the behaviorcan be reproduced by the analysis. In addition, high-frequency parts in the time history are observed particularly in the upper floor in the tests (Figs.10 (c), (d)), but the analysis poorly simulates it. It is considered that high frequency parts is caused by vertical motion of the slab, but the behavior could not be evaluated by the present model.

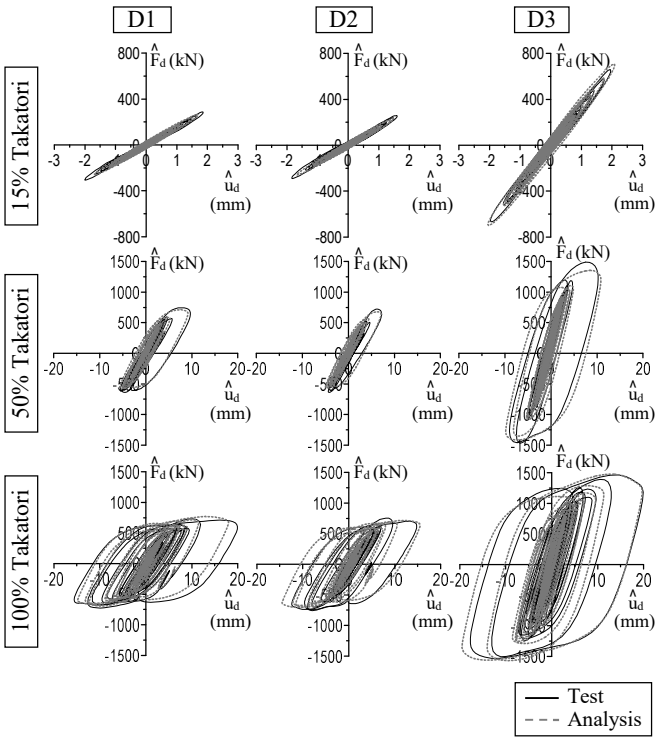

Fig. 7 – Force - deformation relationship of each dampers (1st floor)

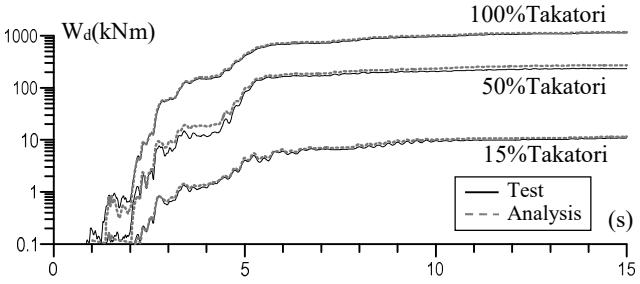

Fig. 8 – Energy absorption of dampers (sum of all dampers)

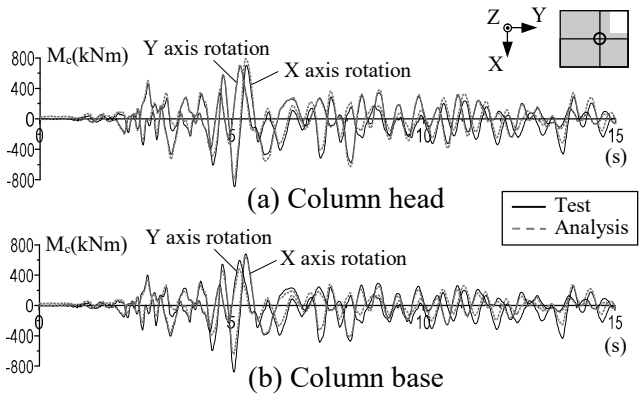

Fig. 9 – Bending moment of 1st floor column (C5, 100%Takatori)

Fig.11 shows the time history of the beam moment. The moment in the three frames where dampers are attached can be evaluated with high accuracy by the analysis. However, in the analysis model, the stiffness of the beam modeled by the line element uses the average of the positive and negative bending stiffness, so the test results tends to be underestimated when the composite beam is subjected to positive bending moment, and vice versa (Figs.11 (b), (c)).

Fig.12 shows the axial force of the composite beam. Unlike the undamped cases, when dampers are attached in the specimen, damping force is transmitted to beams through slab, and axial force is generated in the neighboring beams. In the analysis model used from reference [7] (hereinafter called "past model"), only stiffness against the weak axis bending of beams crossing the center of specimen (X2,Y2 frame) is made rigid, so that the rigid floor assumption is established without restricting the deformation of the beam in the axial direction. However, in the past model, the damper axial force is transmitted to beams directly because the transmission of inertial force through slabs cannot be reproduced, so the composite beam axial force is overestimated by the analysis (Figs.12 (b), (c)), where the test value is the average measured at 2 sections at the position where strain gauge is attached, and the analysis value is the average generated in beam elements in the same span as the specimen.

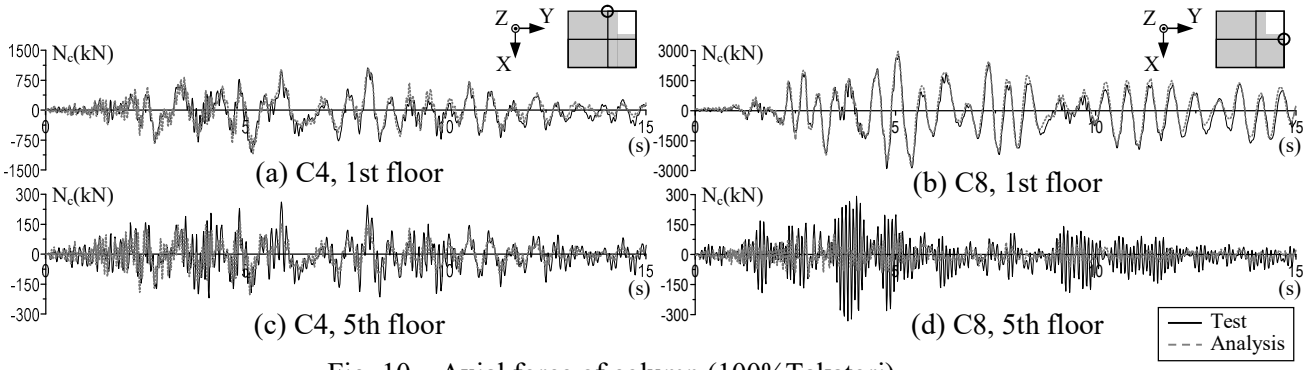

Fig. 10 – Axial force of column (100%Takatori)

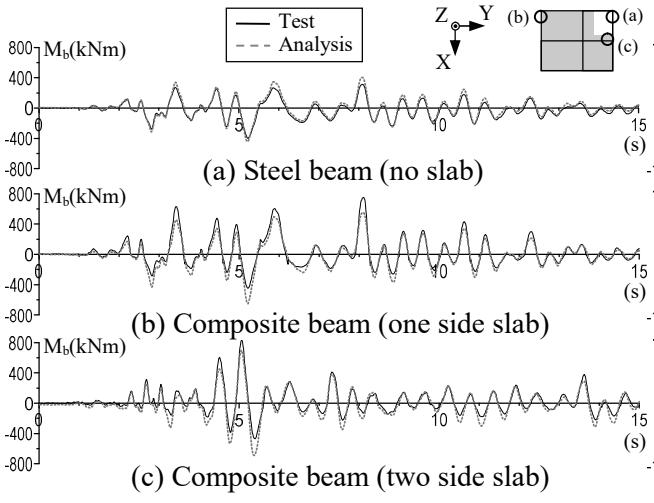

Fig. 11 – Bending moment of composite beam (2nd floor, 100%Takatori)

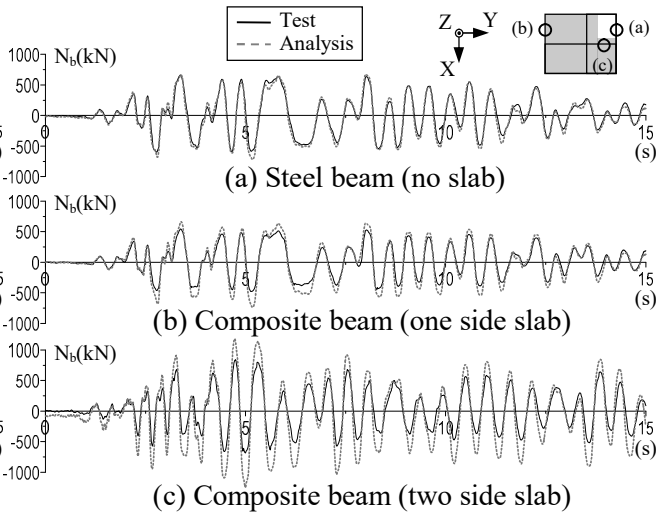

Fig. 12 – Axial force of composite beam (2nd floor, 100%Takatori)

3.3 Modeling of Slab In-plane Flexibility

In this section, the analysis model (hereinafter called "modified model") that reproduces the transmission of inertial force in slabs is used. Specifically, in order to evaluate in-plane shear deformations of slabs, rigid cross truss elements and diagonal truss elements having the shear stiffness of slabs are used in the analysis model as shown in Fig.13. And, although horizontal masses are arranged at intersections of

beams, columns and truss elements according to contributory areas by each, vertical masses are arranged at only intersections of beams and columns.

Fig.14 shows the time history of the axial force of composite beam when the modified model is used. The beam axial force can be accurately evaluated for the beams with or without slab. In order to consider rigid floor assumpion, the analysis was performed with the stiffness of truss elements set to 1000 times. As a result, due to high restraint effects on the beams, the axial force of the beam with one side slab becomes smaller, and that with two side slab is estimated to be almost zero. In the rigid floor assumption, the beam axial force should generally be zero even with one side slab, but, in the analysis, the beam axial force isgenerated in only corner beam (e.g., Fig.13 ②) because only corner column (e.g., Fig.13 ①) cannot be fixed completely by the rigid truss elements. So, the beam axial force of analysis results did not become zero.

Fig.15 shows the time history of the axial force of the steel beam part (excluding the slab). In the tests,it is calculated theoretically from the reference [7], but in the analysis, since steel beam and slab are modeled integrally by line elements, the axial force of steel beam part is obtained by reducing composite beam

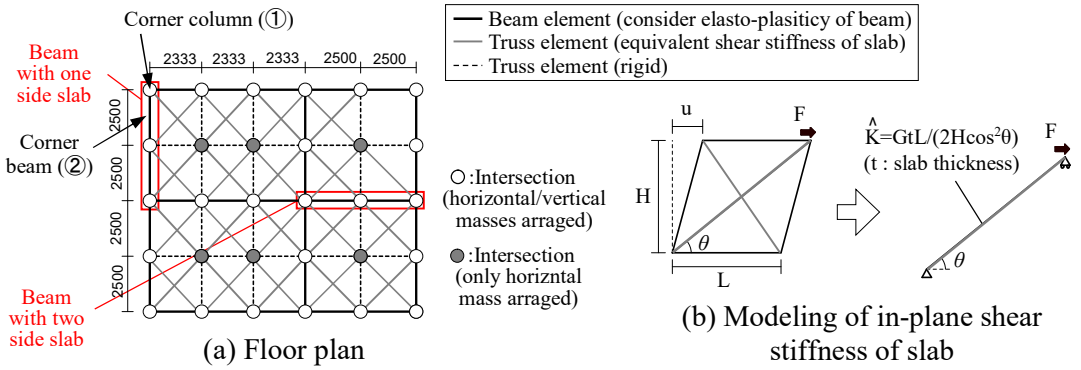

(a) Floor plan (b) Modeling of in-plane shear stiffness of slab

Fig. 13 – Analysis model considering in-plane shear deformation of slabs

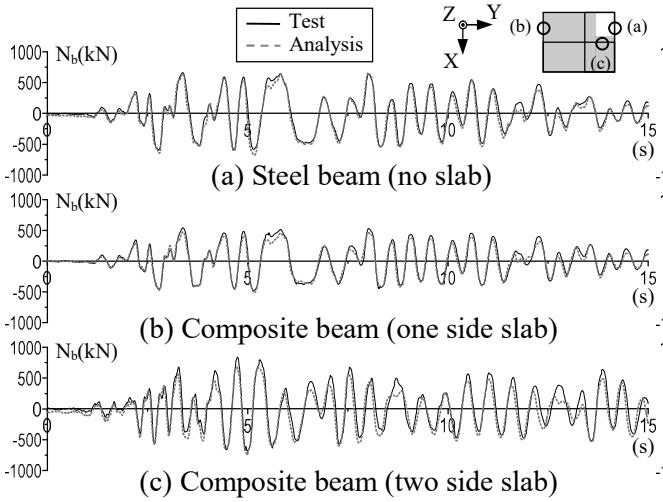

(a) Steel beam (no slab)

(b) Composite beam (one side slab)

(c) Composite beam (two side slab)

Fig. 14 – Axial force of composite beam (modified model, 2nd floor, 100%Takatori)

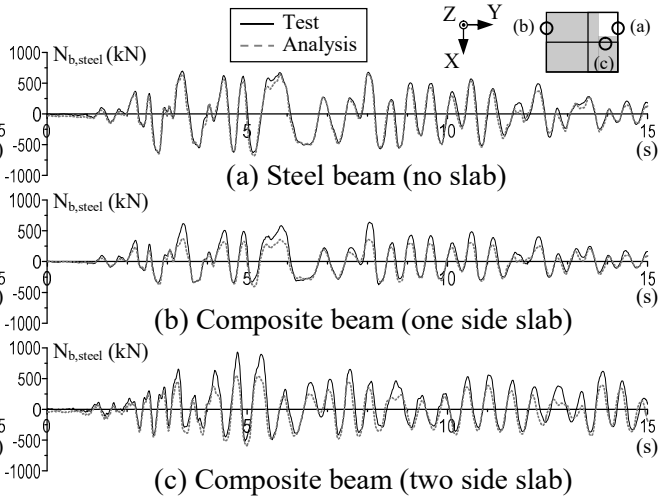

(a) Steel beam (no slab)

(b) Composite beam (one side slab)

(c) Composite beam (two side slab)

Fig. 15 – Axial force of steel beam part (modified model, 2nd floor, 100%Takatori)

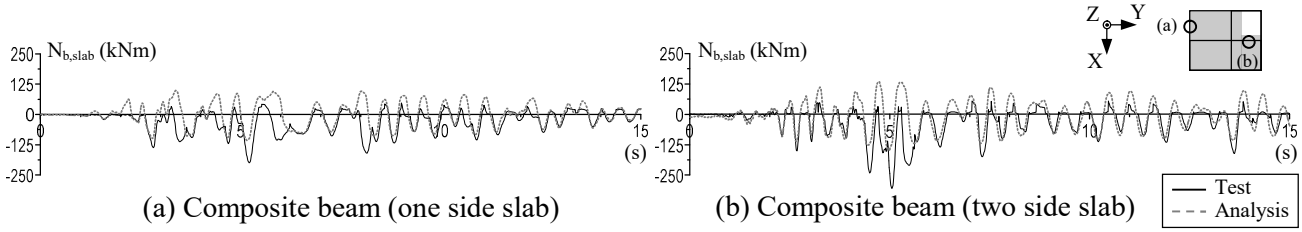

(a) Composite beam (one side slab) (b) Composite beam (two side slab)

Fig. 16 – Axial force of slab part (modified model, 2nd floor, 100%Takatori)

axial force to equivalent area of steel beam. As a result, the evaluation is good throughout, but the axial force of the composite beams (Figs.15 (b), (c)) tended to be slightly smaller on the tension side and slightly larger on the compression side compared to the test results. It is because the analysis do not reflect the difference between tensile stiffness and compressive stiffness of the concrete constituting the slab. Actually, as shown in the time history of the axial force of the slab shown in Fig.16, the axial force is almost the same in tension and compression in the analysis results, on the other hand, the slab bears almost no axial force in tension and bears large axial force in compression in the test results.

Since bending moment and axial force of beams can be evaluated appropriately by the modified model, the test values of the strain data attached to the beam can also be evaluated by the analysis. These following equations (1) and (2) are used as the method.

$$\phi = \frac{M}{I_{cn}E_s}, \quad \varepsilon = \frac{N}{A_{comp}E_s} \tag{1), (2)}$$

where ϕ = curvature of beam due to bending moment, ε = beam strain due to axial force, I_{cn} = equivalent moment of inertia of composite beam, A_{comp} = equivalent cross section of composite beam, E_s = steel Young's modulus. The strain distribution in the cross section is assumed to be flat. Further, I_{cn} and A_{comp} are calculated based on the effective width of the slab used in the analysis model, using the ratio of Young's modulus between steel and concrete.

Fig.17 shows the time history of upper and lower flange strain value of cross section where strain of beams was measured in the tests. Because the neutral axis location moves to the upper flange side due to composite effects of slab, the strain of the lower flange side increases overall. But, in the B58 beam with damper, the upper flange has a relatively large strain particularly in ② section because the neutral axis location shifts downward on the C8 side of the beam due to the axial force generated in the beam. In the analysis, the tendeny can be evaluated with high accuracy.

From the above, the effect of changing the slab thickness can be evaluated by the analysis. Here, focus on the X frames when relative displacement of Y direction from base to top is maximum. Fig.18 shows the shear force distribution of each X frames when the slab thickness, that is, the stiffness of the truss element is changed to 0.2, 0.5, 0.7, 1.5, 2.0, 3.0, and 1000 times. At 15% Takatori motion input, the frame shearing force tended to be smaller as the slab thickness is larger. Since the slab also the function as a linked elements of damper and frame, higher stiffness damper bears relatively large shear force when the stiffness of the slab is higher, and vice versa. At 100% Takatori motion input, the tendency is not so appeared because the equivalent stiffness of the damper becomes lower due to yields of the damper.

Fig.19 shows the tendency of beam axial force due to the change of slab thickness. The beam axial forces of X2 frame (with dampers) are greatly affected by the slab thickness, but the beam axial forces of X1 and X3 frames (without damper) are less affected. In addition, while the effect of slab thickness on the axial force of the beam with damper (B58) become smaller in the upper floor, that of the adjacent beam without damper (B25) become larger in the upper floor. In order to properly evaluate beam axial forces around frames to which damper is attached, it is necessary to modeling the slab stiffness appropriately.

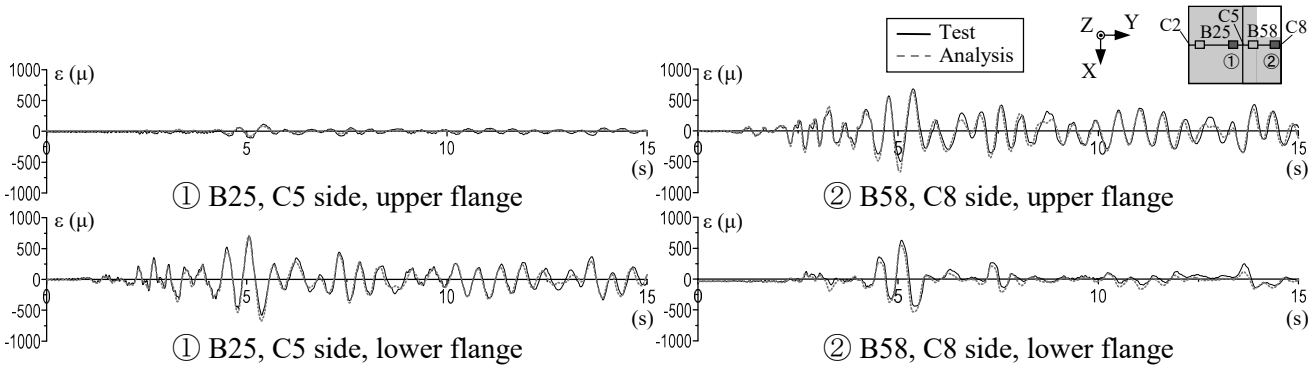

Fig. 17 – Strain of beam flange (modified model, 2nd floor, 100%Takatori)

In this section, we described that local response can be evaluated in more detail by properly modeling slabs. However, modeling of the slab described above did not significantly affect the global and damper responses, and generally slab is assumed to have a rigid floor asssumption in a general design in Japan. So, the modified model is used for the study in this section only, and the past model is used in this report mainly.

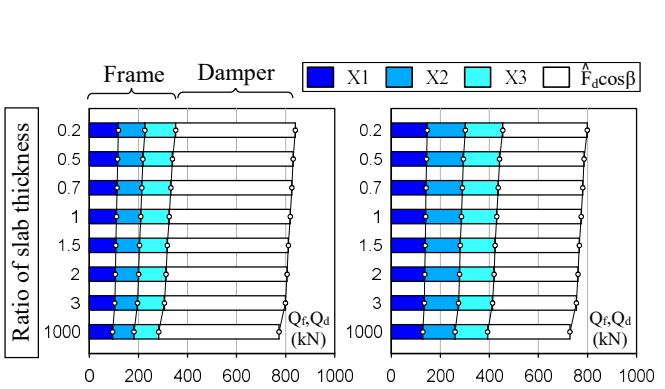

(a) 15%Takatori (left : 3rd floor, right : 2nd floor)

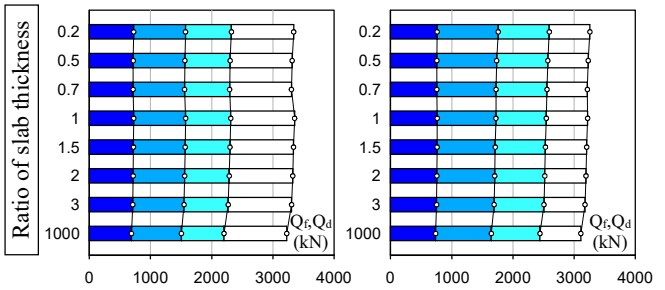

(b) 100%Takatori (left : 3rd floor, right : 2nd floor)

Fig. 18 – Sharing of shear force due to slab thickness (Y direction, when relative displacement from base to top is maximun)

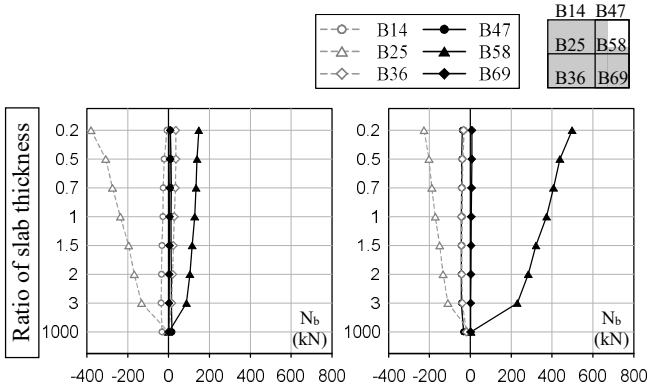

(a) 5th floor (b) 4th floor

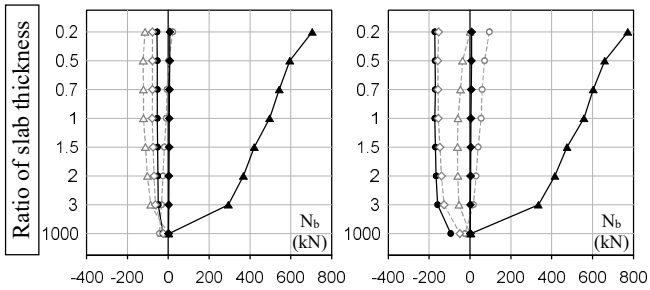

(c) 3rd floor (d) 2nd floor

Fig. 19 – Beam axial force due to slab thickness (100%Takatori, Y direction, when relative displacement from base to top is maximun)

4. Effects of Various Analysis Model on Response Prediction

4.1 Outline of Analysis Model

In this chapter, we consider effects of differences of analysis models on the global response by partially changing the analysis model. Specifically, the analysis model that simulates the tests is defined as ① model, and the study is performed using ② to ⑨ models in which various elements are partially changed. Table 1 shows a summary and 1st mode period of ① to ⑨ models. The mode periods in the X and Y direction of each analysis models are 1.00 to 1.10 times compared to ① model.

Table 1 – Analysis model list

Analysis model description		1st mode period (s)		Ratio to ①	
		X dir.	Y dir.	X dir.	Y dir.
Standard	① Previous analysis model	0.49	0.50	-	-
Change frame model	② Considering beam stiffness only for steel beam	0.52	0.55	1.08	1.10
	③ Do not consider haunches and gusset plates	0.50	0.51	1.02	1.02
	④ Do not consider panel zones	0.49	0.50	1.00	1.00
	⑤ Do not consider non-structural components	0.51	0.53	1.06	1.05
Change damper model	⑥ Do not consider linear viscoelastic element in damper model	0.49	0.50	1.00	1.00
	⑦ Consider only elast-plastic element in damper model	0.49	0.50	1.00	1.00
	⑧ Use damper model with bilinear with maximum damper force equal to steel strength	0.49	0.50	1.00	1.00
	⑨ Use damper model with bilinear with maximum damper force equal to ① model	0.49	0.50	1.00	1.00

※ ⑥ is a model considering only **a** and **b** elements in Fig.2 (c)
⑦ is a model considering only **a** elements in Fig.2 (c)

4.2 Effects on Maximum Response values

Fig.21 shows the dispersion tendency of maximum response value due to difference in frame and damper models. Specifically, this figure shows maximum response values obtained by the analysis of the ① model, maximum and minimum values obtained by the analysis of all models, and average ± standard deviation (σ) obtained by the analysis of all models. Changes in frame models that contribute to stiffness of frames typically tend to make dispersions of the story drift ratio and the story shear force relatively large. But those dispersions become not so large shown in Fig.21 (a) because the range where mode period (T) is 0.49 to 0.55 sec., which is the range of 1st mode periods of ① ~ ⑤ models, is the region where the change of spectrum values is not so large shown in Fig.3. Changes in damper modeling do not change mode periods, but since the amount of energy absorptions of the hysteresis greatly differs for ⑥ ~ ⑨ models (refer to Fig.20), the dispersion of the absolute acceleration becomes relatively large shown in Fig.21 (b).

Fig.22 shows the ratio of the maximum response values of all models to that of ① model. Because the

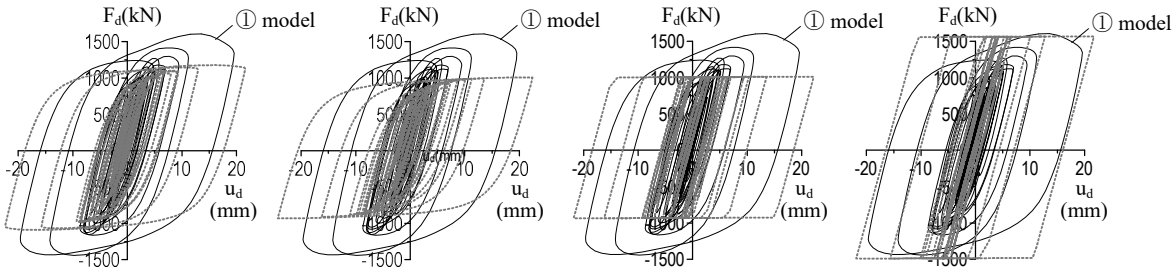

(a) ⑥ model (b) ⑦ model (c) ⑧ model (d) ⑨ model

Fig. 20 – Force - deformation relationship of damper in each models (D3 damper, 1st Floor)

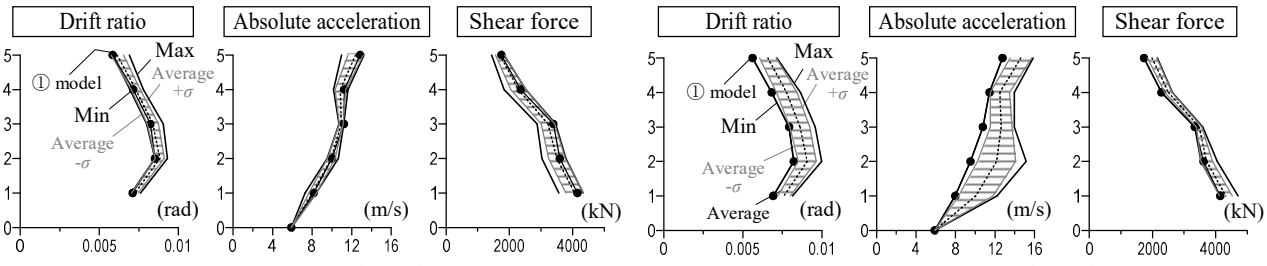

(a) Change frame model (②～⑤ in Table 1) (b) Change damper model (⑥～⑨ in Table 1)

Fig. 21 – Dispersion tendency of maximum response value due to differences in analysis models (100%Takatori, Y direction)

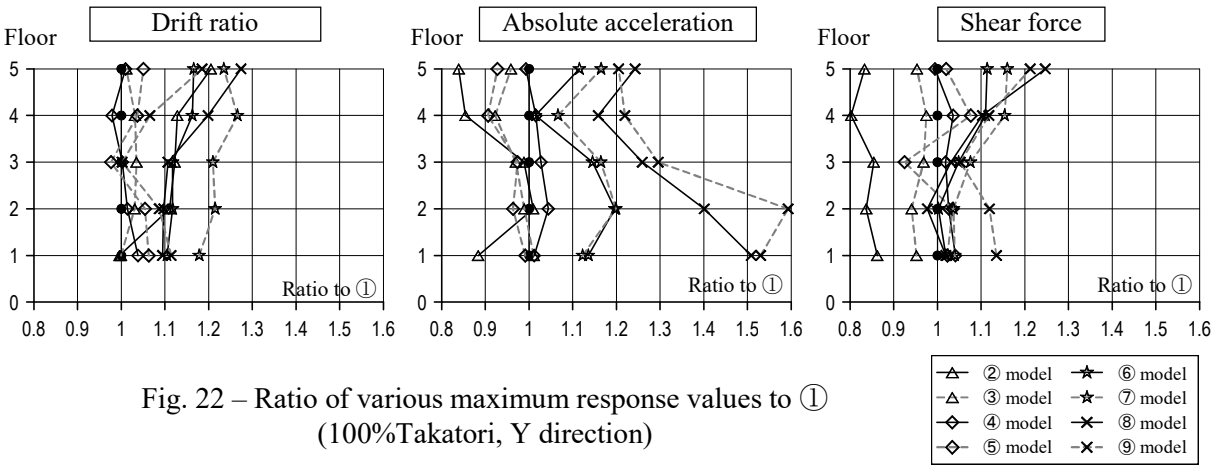

Fig. 22 – Ratio of various maximum response values to ① (100%Takatori, Y direction)

1st mode period of ② model (considering beam stiffness only for steel part) is about 10% larger than that of ① model, the drift ratio is evaluated to be smaller, and absolute acceleration and shear force is evaluated to be larger when ② model is used. The 1st mode period of ⑤ model (do not consider non-structural components) is about 6% larger than that of ① model, but the maximum response value does not change significantly as a result because the non-structural material is modeled so that the stiffness reduced with small amplitude (reference [6]). When ⑥ and ⑦ models (without considering dynamic characteristics of steel damper) are used, the energy absorption of the damper is underestimated, so the maximum response value is larger than the analysis result using ① model. In particular, when ⑧ and ⑨ models (using damper model with bilinear) are used, the absolute acceleration is evaluated about 50% larger. It is desired to properly evaluate damper behaviors by appropriately modeling steel dampers, such as considering dynamic characteristics.

5. Conclusions

In this paper, we focused on 3-D shaking table tests using the full-scale 5-story steel frame building specimen with steel dampers, and it was shown that the test results can be faithfully reproduced from global to local response by using the analysis model proposed in Section 2 (and reference [6]). In addition, we discussed in detail the effect of differences in slab modeling on the analysis results, and we confirmed that it is very important to modeling slabs properly, especially in order to correctly evaluate axial force of beams caused by dampers.

We performed the analysis by partially changing elements of the analysis model. As a result, we confirmed that effects of the stiffness setting of composite beams on global behaviors is relatively large, behavior of steel dampers cannot be accurately evaluated unless analysis considering dynamic characteristics, and absolute acceleration is possibly overestimated by about 50% when using damper model with bilinear used in general design for analysis.

We hope that the finding of the analysis obtained in this study will serve as a reference for analysis in actual design.

6. References

[1] K. Kasai, T. Hikino, H. Ito, Y. Ooki, S. Motoyui, F. Kato, Y. Baba (2011): Overall Test outline and Response of Building without Dampers (3D shake table tests on full scale 5-story steel building with dampers Part 1), J. Struct. Constr. Eng., AIJ, No.663, pp997-1006, (in Japanese).

[2] K. Kasai, Y. Baba, K. Nishizawa, T. Hikino, H. Ito, Y. Ooki, S. Motoyui (2012): Test Results for Building with Steel Dampers (3D Shake Table Tests on Full Scale 5-story Steel Building with Dampers Part2), J. Struct. Constr. Eng., AIJ, No.673, pp. 499-508, (in Japanese).

[3] K. Kasai, Y. Baba, H. Ito, K. Tokoro, T. Hikino, Y. Ooki, R. Murai (2012): 3-D Shake Table Tests on Full Scale 5-story Steel Building with Viscoelastic Dampers, J. Struct. Constr. Eng., AIJ, No.676, pp. 985-994, (in Japanese).

[4] K. Kasai, H. Yamagiwa, Y. Baba, H. Ito, T. Hikino, Y. Ooki (2013): 3-D Shake Table Tests on Full Scale 5-story Steel Building with Oil Dampers, J. Struct. Constr. Eng., AIJ, No.693, pp. 1999-2008, (in Japanese).

[5] K. Kasai, H. Yamagiwa, M. Nishijima, Y. Baba, H. Ito, T. Hikino, Y. Ooki (2014): 3-D Shake Table Tests on Full Scale 5-story Steel Building with Viscous Dampers, J. Struct. Constr. Eng., AIJ, No.695, pp. 47-56, (in Japanese).

[6] K. Kasai, Y. Baba, N. Tetsuta, Y. Sumito (2017): Analytical Study on 3-D Shake Table Test Results for Full-Scale 5-Story Steel Building without Dampers, J. Struct. Constr. Eng., AIJ, No.737, pp. 979-989, (in Japanese).

[7] K. Kasai, K. Matsuda (2014): Full-Scale Dynamic Testing of Response-Controlled Buildings and Their Components: Concepts, Methods, and Findings, Earthq. Eng. & Eng. Vib., Vol.13, pp. 167-181.

[8] K. Kasai, Y. Matsuda (2015): Seismic Behavior of Composite Beams under Damper and Frame Forces of Shifted Phases : Finding from Full-Scale Tests of Buildings and Subassemblies, 6th International Conference on Advances in Experimental Structural Engineering.

[9] K. Kasai, S. Murata, F. Kato, T. Hikino, Y. Ooki (2011): Evaluation Rule for Vibration Period, Damping, and Mode Vector of Buildings Tested by a Shake Table with Inevitable Rocking Motions, J. Struct. Constr. Eng., AIJ, No.670, pp. 2031-2040, (in Japanese).

